Inorganic Chemistry Communications 180 (2025) 115024

Contents lists available at ScienceDirect

Inorganic Chemistry Communications

journal homepage: www.elsevier.com/locate/inoche

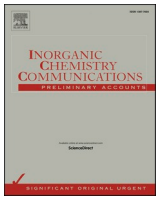

Research Article

Structural variations in copper(II) amine-bisphenolate complexes: Evaluation of *in vitro* antiproliferative activity against human cancer and normal cells

Anssi Peuronen [a], Pia Damlin [b], Ján Vančo [c], Zdeněk Dvořák [d], Zdeněk Trávníček [c,*], Ari Lehtonen [a,*]

[a] Intelligent Materials Chemistry Research Group, Department of Chemistry, University of Turku, FI-20014 Turku, Finland
[b] Materials Chemistry Research Group, Department of Chemistry, University of Turku, FI-20014 Turku, Finland
[c] Regional Centre of Advanced Technologies and Materials, Czech Advanced Technology and Research Institute, Palacký University, Šlechtitelů 27, CZ-779 00 Olomouc, Czech Republic
[d] Department of Cell Biology and Genetics, Faculty of Science, Palacký University, Šlechtitelů 27, CZ-779 00 Olomouc, Czech Republic

ARTICLE INFO

Keywords:
Copper(II) complexes
Amine-bisphenolates
Crystal structures
In vitro cytotoxicity

ABSTRACT

Three copper(II) complexes with variously substituted amine-bisphenolates (H_2L1, H_2L2 and H_2L3) have been prepared. Variation in the composition and structure of the free ligands resulted in the formation of three structurally distinct copper(II) complexes: dinuclear **1**, mononuclear **2** and trinuclear **3**. Various physical techniques were used to characterise the complexes, including single-crystal X-ray analysis and variable-temperature magnetic susceptibility measurements (5–297 K). The compounds were evaluated for their *in vitro* antiproliferative effects against three human cancer cell lines (ovarian A2780 and A2780R, breast MCF7) and normal HaCaT cells. The results showed that both the free ligands and the complexes exhibit strong-to-moderate cytotoxicity. **2** and **3** are significantly more effective against A2780, A2780R and MCF7 cells than the metallodrug cisplatin. The cytotoxicity of complexes **1**–**3** is bound to the cytotoxicity of the free ligands and remains almost unchanged over 24, 48 and 72 h. The copper accumulation in A2780 cells was studied by ICP-MS over 2–72 h of co-incubation of **1**–**3**. Complex **1** caused the highest uptake of copper into A2780 cells, reaching up to 100 times higher Cu concentration compared to untreated cells, while **2** and **3** showed only *ca* 5–10-fold increase of Cu uptake in A2780 cells. No apparent signs of hydrolysis of **1**–**3** in a MeOH/water mixture were observed in mass spectrometry experiments even after 72 h of standing at laboratory temperature. The mass spectrometry-based interaction studies of **1**–**3** with L-cysteine (Cys) and reduced glutathione (GSH) did not show direct evidence of the interaction product formation. Only the signals, corresponding to the free ligands were identified in mass spectra after 24 h and 72 h of incubation.

1. Introduction

The pharmaceutical use of coordination compounds can provide new avenues for the design of drugs with properties which are not available to organic compounds. [1–3] As a well-known example, the use of cisplatin to treat various types of neoplasia has demonstrated the value of metal-based drugs in the treatment of cancer. [4] However, the use of cisplatin is associated with serious side effects such as vomiting, nephrotoxicity, neurotoxicity, bone marrow suppression and hearing loss. [5] These complications have motivated scientists to develop other metal-based drugs, with improved pharmacochemical properties and with different targets. Metal complexes with pharmaceutical properties can be divided into different categories according to their mode of action. For example, the entire complex may be active, the metal ion may be active, or one or more of the ligands may cause biological activity. In general, the different coordination numbers, coordination geometries and oxidation states of the metal centres as well as the different thermodynamic and kinetic properties of the complexes, offer a wide variety of reactivities to be studied. As a result, several coordination compounds of metal ions such as V, Ru, Os, Ir, Au and Cu with a wide range of

* Corresponding authors.
E-mail addresses: anssi.peuronen@utu.fi (A. Peuronen), pia.damlin@utu.fi (P. Damlin), jan.vanco@upol.cz (J. Vančo), zdenek.dvorak@upol.cz (Z. Dvořák), zdenek.travnicek@upol.cz (Z. Trávníček), ari.lehtonen@utu.fi (A. Lehtonen).

https://doi.org/10.1016/j.inoche.2025.115024
Received 27 March 2025; Received in revised form 19 June 2025; Accepted 3 July 2025
Available online 8 July 2025

different ligand structures have been developed as potential antitumor chemotherapeutics. [6–11] For example, copper-based complexes have been investigated on the assumption that endogenous metals may be less toxic to normal cells than exogeneous metals such as platinum. [12].

Hypoxic regions, or areas of reduced tissue oxygenation, are found in many solid tumours due to inadequate blood supply, which can affect cellular metabolism and signalling pathways. Consequently, tumour hypoxia can be exploited to develop new drug molecules that are activated in the reducing environment of cancer cells. In this environment, copper becomes very attractive as it can exist in two different oxidative states in living cells. The physiological concentration of copper in the body is regulated by a number of mechanisms involving the liver ceruloplasmin and albumin, as well as copper transport proteins. [13] However, in excess, copper can be toxic to normal cells due to the formation of reactive oxygen species (ROS) or reactive nitrogen species (RNS). Under hypoxic conditions, Cu(II) can be reduced to Cu(I), a process that can lead to the formation of ROS and RNS. The accumulation of ROS can lead to oxidative stress, which can damage cellular components and activate pathways that trigger apoptosis. Cancer cells often resist apoptosis, but increased oxidative stress can overwhelm these mechanisms and lead to cell death. As cancer cells have shown increased Cu uptake, Cu compounds are expected to be less toxic to normal cells, while retaining effective cytotoxicity against cancer cells. [14,15].

Amine bisphenols with pendant-arm donors are versatile ligands that coordinate to the metal ions in a tripodal fashion. The coordination geometry of the metal centre can be modified by the ligand design. In particular, the *ortho*-substituents of the phenolate moieties and the nature of the pendant arm donor influence the structure and reactivity of the complexes. Depending on the metal ion and the ligand structure, the complexes formed can be monomeric, dimeric or oligomeric.[16] Among them, Cu(II) amine-bisphenolates are intriguing compounds, exhibiting various functional properties and biological activities. These complexes have been extensively studied for their interesting magnetic properties [17–23], as well as their role as phosphotriesterase mimics [24] and structural models for galactose oxidase [25,26]. In addition, Cu (II) amine-bisphenolates have shown promising anticancer potential, with certain complexes exhibiting even higher cytotoxicity than the widely used chemotherapeutic drug cisplatin.[27] This unique combination of chemical versatility and biological activity makes them valuable candidates for further investigation. In this article, we report three new Cu(II) complexes with amine-bisphenolates bearing a dangling OH group in the pedant arm of the ligand structure. The in vitro cytotoxicity of the Cu(II) complexes and their corresponding free ligands was evaluated against selected human cancer and normal cell lines.

2. Results and discussion

2.1. Syntheses

The ligand precursors were prepared or according to the method published previously for the synthesis of **H_2L3**. [28] The 1:2:2 mixture of 2-(2-aminoethoxy)ethan-1-ol, paraformaldehyde and 2,4-disubstituted phenols was heated at 125 °C for four hours, followed by crystallisation. The ligand precursors were allowed to react with copper(II) perchlorate in basic MeOH solutions to give dark brown-red mixtures, which were stored at room temperature for two days (Scheme 1). The volatiles were then removed, and the residues were crystallised from MeOH (**1**,**2**) or *n*-hexane (**3**) to give dark crystals in about 50–65 % non-optimised yield. All complexes are soluble in DMSO and moderately soluble in MeOH and acetonitrile. **2** and **3** are also soluble in dichloromethane, whereas **1** is only slightly soluble. As shown by the XRD analyses (see below), **1** crystallises as a dimeric complex, **2** crystallises as a monomeric MeOH adduct with three molecules of solvent in the crystal lattice, and **3** is found in the solid state as a combination of monomeric and dimeric species with one molecule of *n*-hexane in the lattice. It is interesting to note that non-crystalline **3** is readily soluble in *n*-hexane.

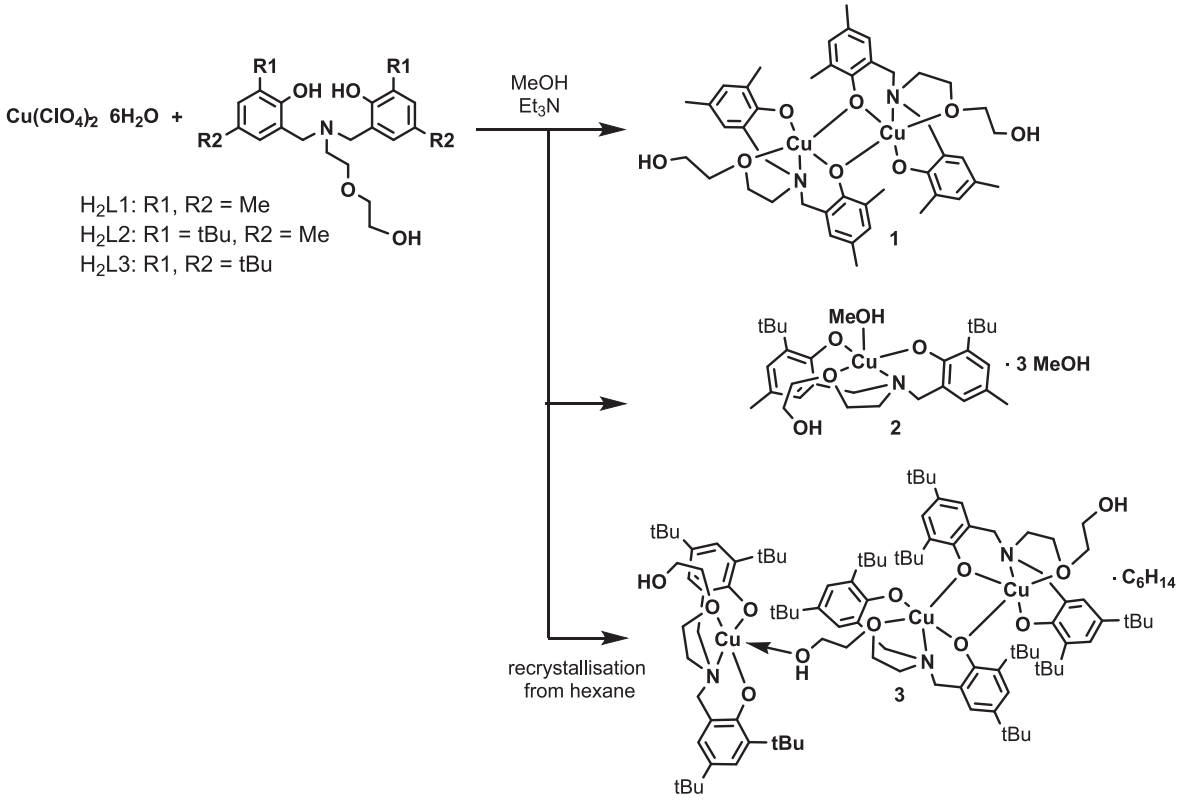

Scheme 1. Syntheses of the Cu(II) complexes.

2.2. Structural characterisation of complexes 1–3

The molecular structures of the Cu(II) complexes were determined by single-crystal X-ray diffraction, and their crystal data and structure refinements are given in Table S1 in Supporting Information. Compound **1** crystallises from MeOH solution as symmetric dinuclear units $[Cu_2L1_2]$ in which the ligands coordinate as tetradentate O_2NO donors. As one deprotonated phenolic oxygen acts as a bridging atom bonded to the neighbouring Cu, the donor set around each of the Cu atoms is NO_4, showing pentacoordination around each Cu. The phenolic OH groups have been deprotonated while the OH in the pendant arm remains intact. The two Cu centres are linked by two phenolate oxygens, forming a four-membered symmetrical rectangular Cu_2-(μ-$O_{Phenolate}$)$_2$ core (Fig. 1). The ligand acts as a dianion, coordinating in a tetradentate and bridging manner through the two deprotonated phenolic oxygen atoms and the neutral oxygen and nitrogen donors of the amino alcohol group. The Cu–O and Cu–N distances are typical for the corresponding amine-bisphenolate complexes. [17,19–22,27] Generally, the coordination geometries of the pentacoordinated Cu(II) complexes fall between the ideal square-pyramidal and trigonal-bipyramidal structures. These geometries are described by the parameter τ. [29] For **1**, the $O_{Phenolate}$-Cu-$O_{Phenolate}$ angle is 167.2° and the N-Cu-O_{Ether} angle is 147.6°. The τ value of 0.33 suggests the distorted tetragonal pyramidal geometry for Cu(II) ions. The dangling OH group in the pendant arm forms an intramolecular hydrogen bond to the $O_{Phenolate}$ with an H···O distance of 1.873 Å and an O-H-O angle of 171.8°. Complex **2** crystallises from MeOH as a mononuclear complex together with three solvent molecules in the crystal lattice. The amine-bisphenolate ligand coordinates as a tetradentate O_2NO donor while the fifth coordination site is occupied by a MeOH molecule (Fig. 1). The τ value calculated from N-Cu-O_{MeOH} and $O_{Phenolate}$-Cu-$O_{Phenolate}$ (167.0° and 155.9°, respectively) is 0.18, so the Cu(II) ion has a distorted tetragonal pyramidal coordination geometry. The crystallisation of **3** from MeOH or other polar solvents proved difficult, but it crystallises from *n*-hexane as trinuclear clusters, which are formed from covalently connected mononuclear and dinuclear units. The overall structure of the dimeric moiety is similar to that of **1**, while the coordination sphere in the monomeric moiety is related to that of **2**. A dangling OH from the dimeric moiety coordinates to the mononuclear moiety's Cu(II) ion (Fig. 3). In the dinuclear unit, the four-membered ring adopts a "butterfly" shape, while the Cu-O-Cu-O torsion angle is 45.5°. For Cu1, the $O_{Phenolate}$-Cu-$O_{Phenolate}$ angle is 166.3° and the N-Cu-O_{Bridge} angle is 150.6°, giving a τ value of 0.26 for a distorted tetragonal pyramid. Similarly, for Cu2 the $O_{Phenolate}$-Cu-$O_{Phenolate}$ and N-Cu-O_{Bridge} angles are 168.0° and 153.1°, respectively, giving a τ value of 0.28 for a

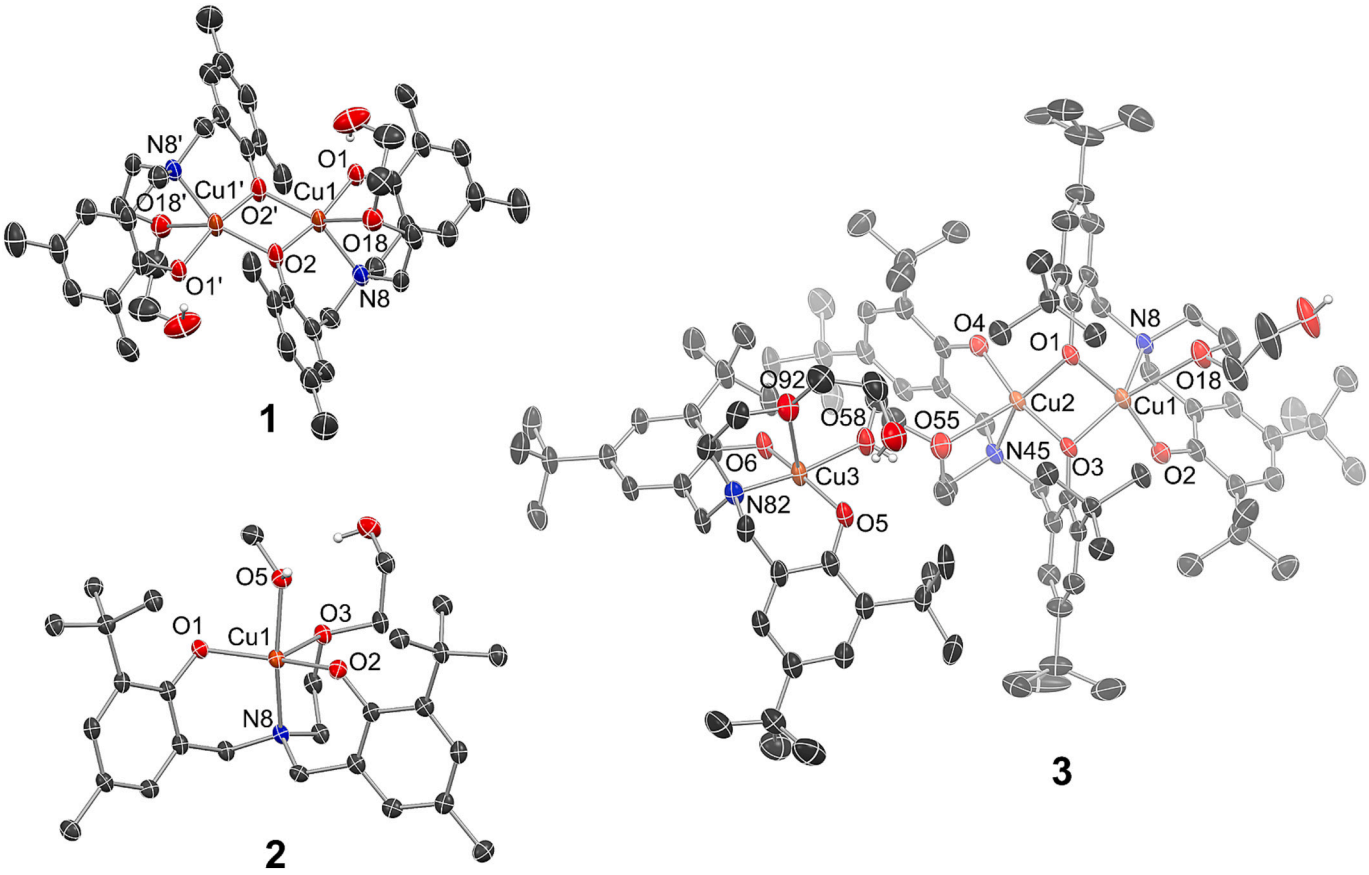

Fig. 1. The molecular structures of **1** (top left), **2** (bottom left) and **3** (right) obtained by single crystal X-ray diffraction. Displacement ellipsoids are presented at the 50 % probability level. The C—H hydrogens and solvent molecules are omitted for clarity. List of selected interatomic distances (Å) and angles (°) for **1** ('1-x,1-y,1-z): Cu1–Cu1' = 3.0531(9), Cu1–O1 = 1.897(3), Cu1–O2 = 1.931(3), Cu1–O2' = 1.975(3), Cu1–N8 = 2.015(4); Cu1–O2–Cu1' = 102.8(1), O1–Cu1–O2' = 95.6(1), O1–Cu1–O2 = 167.2(1), O1–Cu1–N8 = 97.0(1), O1–Cu1–O18 = 88.6(1), O18–Cu1–N8 = 76.7(1), N8–Cu1–O2 = 94.5(1), N8–Cu1–O2' = 174.6(1); for **2**: Cu1–O1 = 1.9237(17), Cu1–O2 = 1.8769(17), Cu1–O3 = 2.5327(17), Cu1–O5 = 2.0331(18), Cu1–N8 = 2.042(2); O1–Cu1–O3 = 102.8(1), O1–Cu1–O5 = 89.45(7), O1–Cu1–N8 = 94.23(8), O2–Cu1–O1 = 155.9(1), O2–Cu1–O3 = 100.6(1), O2–Cu1–O5 = 85.9(1), O2–Cu1–N8 = 95.6(1), O5–Cu1–O3 = 88.3(1), O5–Cu1–N8 = 167.0(1), N8–Cu1–O3 = 78.8(1); for **3**: Cu1–Cu2 = 2.7294(7), Cu1–O1 = 1.949(3), Cu1–O2 = 1.873(3), Cu1–O3 = 2.033(2), Cu1–N8 = 2.040(3), Cu2–O1 = 2.020(2), Cu2–O3 = 1.960(2), Cu2–O4 = 1.878(3), Cu2–N45 = 2.039(3), Cu3–O5 = 1.924(3), Cu3–O6 = 1.886(3), Cu3–O58 = 2.042(3), Cu3–N82 = 1.989(3); O1–Cu1–O3 = 74.4(1), O1–Cu1–N8 = 93.7(1), O2–Cu1–O1 = 166.3(1), O2–Cu1–O3 = 92.0(1), O2–Cu1–N8 = 97.3(1), O3–Cu1–N8 = 150.6(1), O1–Cu2–N45 = 153.0(1), O3–Cu2–O1 = 74.5(1), O3–Cu2–N45 = 93.3(1), O4–Cu2–O1 = 93.7(1), O4–Cu2–O3 = 168.1(1), O4–Cu2–N45 = 96.8(1), O5–Cu3–O58 = 83.6(1), O5–Cu3–N82 = 97.1(1), O6–Cu3–O5 = 161.3(1), O6–Cu3–O58 = 88.8(1), O6–Cu3–N82 = 93.8(1), N82–Cu3–O58 = 168.7(1), Cu1–O1–Cu2 = 86.9(1).

distorted tetragonal pyramidal geometry. In contrast, the Cu3 in the monomeric part has a tetragonal pyramidal coordination geometry, the τ value calculated from N-Cu-$O_{alcohol}$ and $O_{Phenolate}$-Cu-$O_{Phenolate}$ (168.8° and 161.3°, respectively) is 0.09. The coordination geometries were also analysed using Continuous Shape Measures (CShM) calculations where the spatial arrangement of the ligand donor atoms around the Cu centre is compared to a set of reference polyhedra. [30] According to the CShMs (Table S2 in Supporting Information) the coordination geometry of complex **1** can be described as a trigonal bipyramid or spherical square pyramid, as the corresponding CShMs are almost identical, while their values suggest distortion from the respective ideal coordination polyhedra. For **2**, the best fit is displayed by trigonal bipyramid. In contrast, the three distinct Cu-centres in complex **3** are all best described by a spherical square pyramid. However, a comparison of the CShMs reveals that their geometries differ, with increasing distortion from the ideal spherical square pyramidal geometry in the sequence Cu3 > Cu2 > Cu1.

The ligand backbone structure and tripodal coordination mode are similar in all the compounds studied, as the variations are in the substituents of the phenolic moieties. Specifically, there are methyl substituents in the *ortho*-positions of the phenolates in **1**, whereas in **2** and **3**, there are methyl substituents in the ortho-positions of the phenolates, whereas in **2** and **3**, the substituents close to the metal centres are *tert*-butyl groups. Therefore, one might expect the solid-state structures of these complexes to be very similar. However, **1** crystallises from MeOH as phenolate-bridged dimers, **2** crystallises as mononuclear MeOH adducts, while **3** does not crystallise from MeOH; instead, it crystallises from *n*-hexane to combine mononuclear and dinuclear units. We can assume that there are some equilibria between mononuclear and dinuclear species in the solutions and that the precipitation of different crystals is mainly based on different crystal packing forces and weak intramolecular interactions.

2.3. Magnetic properties of complexes *1*–*3*

The measurements of the temperature dependence of magnetic susceptibility of complexes **1**–**3** through the temperature interval of 5–297 K at B = 0.1 T were used to reveal the magnetic features of the complexes. At first, the temperature dependencies of the effective magnetic moments per 1 Cu atom were visualised (see Figs. S1–S3 in Supporting Information). It can be clearly seen from the dependencies that the values of μ_{eff}/μ_B fall nearly linearly from 1.44 (297 K) to 0.40 (5 K) for the dinuclear complex **1,** indicating strong antiferromagnetic coupling between two copper(II) ions. On the other hand, the μ_{eff}/μ_B values lie in a nearly linear line in the mononuclear complex **2**, varying from 1.83 (297 K) to 1.95 (5 K), and representing behaviour of a diluted paramagnetic compound obeying the Curie-Weiss law [31], with the following best-fit parameters: $C = 0.476$ cm^3 mol^{-1} K, $\theta = 0$ K, and TIP $= 6.716 \times 10^{-4}$ cm^3 mol^{-1}, see Fig. S4 in Supporting Information. In the case of the trinuclear complex **3**, the μ_{eff}/μ_B values decrease gradually from 297 K ($\mu_{eff}/\mu_B = 1.94$) with decreasing temperature to $\mu_{eff}/\mu_B =$ 1.86 at *ca* 32 K, while consequently they fall to the value of 1.63 μ_{eff}/μ_B (5 K). This behaviour suggests an antiferromagnetic coupling in complex **3**. Consequently, the magnetic data of complexes **1** and **3** were evaluated using the PHI software package [32]. The best-fit parameters were found as follows: $J = -209$ (1) cm^{-1}, g_1(Cu1) = 2.17 (3), g_2(Cu2) = 2.20(0), ⁎J $= -0.05$ cm^{-1}, TIP (temperature independent paramagnetism) = 0.53 $\times 10^{-3}$ cm^3 mol^{-1}, and IMP (monomeric impurity) = 0.4 % (for **1**); and $J_1 = -19.9$ (9) cm^{-1}, $J_2 = -2.37$ (6) cm^{-1}, g_1(Cu1) = 1.92 (3), g_2(Cu2) = 2.26 (2), g_3(Cu3) = 2.30(0), ⁎$J = -0.01$ cm^{-1}, TIP $= 0.36 \times 10^{-3}$ cm^3 mol^{-1} (for **3**). The temperature dependencies of $\chi_M T$, χ_M and $1/\chi_M$ for complexes **1** and **3**, together with the best-fit curves, are shown in Figs. S5–S10 in Supporting Information.

Based on the molecular structure of complex **1**, it belongs to a family of phenoxo-bridged dinuclear copper(II) complexes. The structural and magnetic features of this group are described and correlated in the literature very well, as demonstrated by a few published review papers [33–35]. The magnetic features of such systems can be predicted mainly based on the Cu–O–Cu angle, with its critical value of ca 97°. This value is governed by a degree of overlap between the 3d orbital of copper and the oxygen 2p orbitals of the bridging phenoxo group. Generally speaking, a smaller Cu–O–Cu angle can lead to less effective orbital overlap, resulting in weaker exchange interactions, and vice versa, larger Cu–O–Cu angles can strengthen orbital overlap, leading to stronger antiferromagnetic coupling. This relationship is consistent with the Goodenough–Kanamori rules, which predict the sign and strength of the exchange interactions based on orbital overlap and geometry, as described in greater detail in the above-cited reviews.

In complex **1**, the value of 102.77° was observed for the Cu–O–Cu angle with the separation of Cu···Cu of 3.053 Å, which favours a strong antiferromagnetic exchange, and the calculated value of the exchange integral $J = -209$ cm^{-1} clearly confirms the prediction. On the other hand, the Cu1···Cu2 separations in complex **3** are of 2.729 Å (in the bis (μ-phenoxo) moiety, with the Cu–O–Cu angles of 86.26 and 86.84°) and 7.220 Å (for Cu2···Cu3). Moreover, a degree of deformation in the vicinity of the copper atoms involved in the Cu_2(μ-phenoxo)$_2$ moiety is dissimilar between complexes **1** and **3**, as can be demonstrated by different bond lengths and angles observed in both complexes, which may also point out the differences in orbital overlaps, responsible for the degree of magnetic exchange interactions. Thus, complex **3** revealed moderate antiferromagnetic exchange between Cu1 and Cu2 ions (with $J_1 = -19.9$ (9) cm^{-1}) and a weak antiferromagnetic exchange going through the Cu2···Cu3 pathway (with $J_2 = -2.37$ (6) cm^{-1}). The obtained results are in accordance with those presented in the literature [33].

2.4. Electrochemistry

Cyclic voltammograms for **1**–**3** were measured in DMSO solutions using an Ag/AgCl reference electrode (see Figs. S38–S40). The voltammograms show quasi-reversible redox processes at −0.225 V, −0.175 V and − 0.250 V for **1**, **2** and **3**, respectively, corresponding to the Cu^{2+}/Cu^{+} reduction. The chemically irreversible nature of these processes suggests the instability of the reduced species. There are also two anodic oxidation processes, which are probably due to ligand-centred redox processes, whereby the phenolate group yields a phenoxyl radical in the complex. The cyclic voltammograms of complexes **1**–**3** and the table of related redox potentials are summarised in Supporting Information, see Figs. S38–S40 and Table S3. The values of half-wave potentials ($E_{1/2}$ ranging from −0.175 to −0.250 V) fall within the "Biological Redox Window" as suggested by Peña Q. et al. [36], in which copper(II) complexes are likely to interact with the biomolecules, such as NADH and GSH and thus influence the redox balance within the cells. The imbalance between the intracellular oxidants and antioxidants can lead to the formation of oxidative stress and cellular death [37]. For some specific types of copper(II) complexes, such as *Casiopeínas*, the quantitative structure-activity relationship (QSAR) analyses showed the direct correlation between the half-wave potential and antiproliferative activity/cytotoxicity of the complexes, leading to the hypothesis that more positive half-wave potentials are more favourable for the efficient reduction of Cu(II) to Cu(I) and its participation in Fenton-like processes, and formation of reactive oxygen species (ROS) [38]. Nevertheless, this correlation cannot be generalised for all copper(II) complexes, especially for complexes **1**–**3**, bearing different structural scaffolds.

2.5. In vitro cytotoxicity studies

The *in vitro* cytotoxicities of **1**–**3** were evaluated on three human cancer cell lines, namely: ovarian A2780, ovarian cisplatin-resistant A2780R and breast MCF7. The obtained results, summarised in Table 1, show that complex **1** demonstrates moderate cytotoxicity on

Table 1
In vitro cytotoxicity of copper(II) complexes **1**–**3**, free ligands H_2Lx (x = 1–3), $Cu(ClO_4)_2{\cdot}6H_2O$ (**4**) and cisplatin on ovarian (A2780), cisplatin-resistant ovarian (A2780R) and breast (MCF7) human cancer cell lines, and healthy keratinocyte cells (HaCaT). Data are expressed as IC_{50} ± SD in μM (MTT method, 24 h incubation time).

Compound	IC_{50} ± SD [μM]							
	A2780	A2780R	MCF7	HaCaT	RF*	SI†	SI†† (A2780R)	SI†††
Complex **1**	32.6 ± 4.8	46.2 ± 1.9	25.5 ± 3.2	>50	1.4	>1.5	>1.0	>2.0
Complex **2**	7.5 ± 1.9	10.0 ± 0.5	11.9 ± 3.1	18.4 ± 2.6	1.3	2.5	1.9	1.6
Complex **3**	3.3 ± 0.6	3.7 ± 0.7	3.8 ± 1.6	18.1 ± 3.3	1.1	5.5	4.9	4.8
H_2L1 (ligand for **1**)	24.5 ± 2.6	46.1 ± 2.6	41.0 ± 3.5	>50	1.9	>2.0	>1.1	>1.2
H_2L2 (ligand for **2**)	9.4 ± 1.7	12.8 ± 0.6	17.7 ± 1.8	21.4 ± 2.7	1.4	2.3	1.7	1.2
H_2L3 (ligand for **3**)	9.9 ± 2.0	12.7 ± 3.3	33.2 ± 5.7	>50	1.3	>5.0	>3.9	>1.5
$Cu(ClO_4)_2{\cdot}6H_2O$ **4**	>50	>50	>50	>50	i.c.	i.c.	i.c.	i.c.
Cisplatin	15.4 ± 0.3	>50	37.2 ± 3.3	>50	>3.2	>3.2	i.c.	>1.3

Note: *RF - resistance factor, calculated as the ratio between the IC_{50} value of the resistant cell and the sensitive one IC_{50}(A2780R)/IC_{50}(A2780). †,††,†††SI - selectivity index expressed as IC_{50}(HaCaT)/IC_{50}(A2780†, A2780R††, and MCF7†††, respectively). i.c. = impossible to calculate.

ovarian and breast cell lines, relatively comparable to metallodrug cisplatin, while complexes **2** and **3** reveal significant cytotoxicity with IC_{50} values of 3.3–11.9 μM. However, as seen from the table, the cytotoxicity of complexes **1** and **2** is probably due to the cytotoxicity of the free ligands. Indeed, the IC_{50} values of these complexes and their corresponding organic ligands **H_2L1**, and **H_2L2**, respectively, on A2780 and A2780R cells are similar. In the case of complex **3**, its cytotoxicity is ca. 3 times higher on A2780 and A2780R cells and ca. 9 times higher on MCF7 cells than that of the free ligand. The overall results revealed that complexes **1**–**3** display good resistance factors (RF), calculated as the ratio between the IC_{50} value of the resistant cell line and the sensitive one, i.e. RF = IC_{50}(A2780R)/IC_{50}(A2780), with RF = 1.4, 1.3, and 1.1, respectively. Moreover, the values of the selectivity index (SI), expressed as SI = IC_{50}(HaCaT)/IC_{50}(A2780) reached the best value of 5.5 for complex **3**. Notably, complex **3** showed significantly higher cytotoxicity, resistance and selectivity against the utilised cell lines than cisplatin.

The time-dependent profile, which covers 24 to 72 h, was chosen to evaluate the compounds' cytotoxicity on the selected A2780 cells more deeply. The obtained data are shown in Table 2, and they point out that the cytotoxicity of complexes **1**–**3** and free ligands remains nearly constant with time increase, contrary to cisplatin, where a typical decrease of IC_{50} values can be seen.

2.6. Cellular uptake of copper in A2780 cells

Intracellular copper levels in A2780 cells, incubated with the half-cytotoxic concentrations of complexes **1**–**3** and $Cu(ClO_4)_2{\cdot}6H_2O$ (**4**), were determined at various time points (2, 6, 12, 24, 48 and 72 h) by means of an inductively coupled plasma mass spectrometry (ICP-MS). The cells treated with the vehicle were used as a reference. The intracellular copper levels in A2780 cells (see Fig. 2) were most strongly increased by complex **1**, which carries the least lipophilic ligands and gained the fastest maximum already at 2 h after the application, reaching up to 100 times the normal copper concentration measured in vehicle-only control cells. The concentration of copper decreased slowly, reaching a level 30–40 times higher than that of control cells after 12 h and remained in this range for up to 72 h after the application of the complex. The ionic compound, copper(II) perchlorate hexahydrate, revealed the less effective cellular uptake, which caused a steady increase of the intracellular concentration of copper in A2780 cells up to the maximum after 48 h at *ca* 30 times higher level than in control cells. Complex **2**, which contains the second most lipophilic ligand, caused an almost linear increase in the intracellular copper levels in A2780 cells, reaching a maximum at ca. 10-fold higher concentration as compared to the control cells. Complex **3**, containing the most lipophilic ligand $L3^{2-}$, caused a rapid uptake of copper into A2780 cells, which remained stable in the range of *ca* 5–10 times higher than that of control cells.

Table 2
The time-dependent (24, 48 and 72 h) *in vitro* cytotoxicity of copper(II) complexes **1**–**3**, free ligands H_2Lx (x = 1–3), $Cu(ClO_4)_2{\cdot}6H_2O$ (**4**) and cisplatin on the ovarian A2780 cell line. Data is expressed as IC_{50} ± SD in μM (MTT method).

Compound	Incubation time (A2780 cell line, IC_{50} ± SD [μM])		
	24 h	**48 h**	**72 h**
Complex **1**	32.6 ± 4.8	32.2 ± 1.2	35.2 ± 0.9
Complex **2**	7.5 ± 1.9	8.6 ± 2.1	10.1 ± 1.2
Complex **3**	3.3 ± 0.6	2.7 ± 0.3	2.9 ± 0.4
H_2L1 ligand for **1**	24.5 ± 2.6	28.3 ± 3.7	31.4 ± 3.1
H_2L2 ligand for **2**	9.4 ± 1.7	12.2 ± 0.9	15.1 ± 1.1
H_2L3 ligand for **3**	9.9 ± 2.0	11.8 ± 2.0	12.4 ± 2.1
$Cu(ClO_4)_2{\cdot}6H_2O$ **4**	>50	>50	>50
Cisplatin	15.4 ± 0.3	6.5 ± 3.2	3.7 ± 0.2

2.7. Stability studies of complexes *1*–*3* in a water/MeOH mixture

Hydrolysis of complexes **1**–**3** was investigated by comparing the electrospray ionisation (ESI) mass (MS) spectra of complexes prepared in a water-containing medium (MeOH:H_2O; 1:1 *v*/v) after 24 h of standing at laboratory temperature with the mass spectra of freshly prepared solutions in MeOH. Under the conditions of ESI, the mass spectra of the complexes **1**–**3** in MeOH (see Figs. S11, S14, and S17 in Supporting Information) revealed the presence of two main types of signals of pseudomolecular ions, first corresponding to the released ligand $[H_2L + H]^+$ (i.e. $[H_2L1 + H]^+$ at m/z = 374.24 for **1**; $[H_2L2 + H]^+$ at m/z = 458.34 for **2**; and the $[H_2L3 + H]^+$ at m/z = 542.48 for **3**), and the second one to the monomeric complex unit $[CuL + H]^+$ or $[CuL + Na]^+$ (i.e. $[CuL1 + Na]^+$ at m/z = 457.09 for **1**; $[CuL2 + H]^+$ at m/z = 519.24 for **2**; and $[CuL3 + H]^+$ at m/z = 603.30 for **3**). In the solutions involving the mixture of MeOH:H_2O, no apparent hydrolysis products were identified in the mass spectra after 24 h (see Figs. S12, S15, and S18 in Supporting Information) and after 72 h (see Figs. S13, S16, and S19 in Supporting Information). The main signals, derived from the free ligands and complexes (i.e. $[H_2L + H]^+$ or $[H_2L + Na]^+$ and $[CuL + H]^+$ or $[CuL + Na]^+$), remained unchanged. The stability of the complexes was also investigated by mass spectrometry. The spectra of complexes **1**–**3** were measured in MeOH solutions and water/MeOH mixtures on fresh samples and after 24 h. No changes in the spectra were observed, indicating that all compounds are hydrolytically stable at room temperature.

To determine the stability of the complexes in DMSO and MeOH solvents, their UV–Vis spectra were measured and compared with those of the solid-state ones (see Figs. S20-S22 in Supporting Information). It can be concluded for complex **1** that its DMSO and MeOH spectra are very similar, showing comparable maxima, while the maxima in the solid-state spectra are shifted significantly. This may point out the influence of solvent molecules on the coordination changes in the vicinity of the copper atoms, probably associated with the coordination of these solvent molecules to copper. This interpretation can be supported by the X-ray structure of the dinuclear complex **1** (see Fig. 1), where the Cu

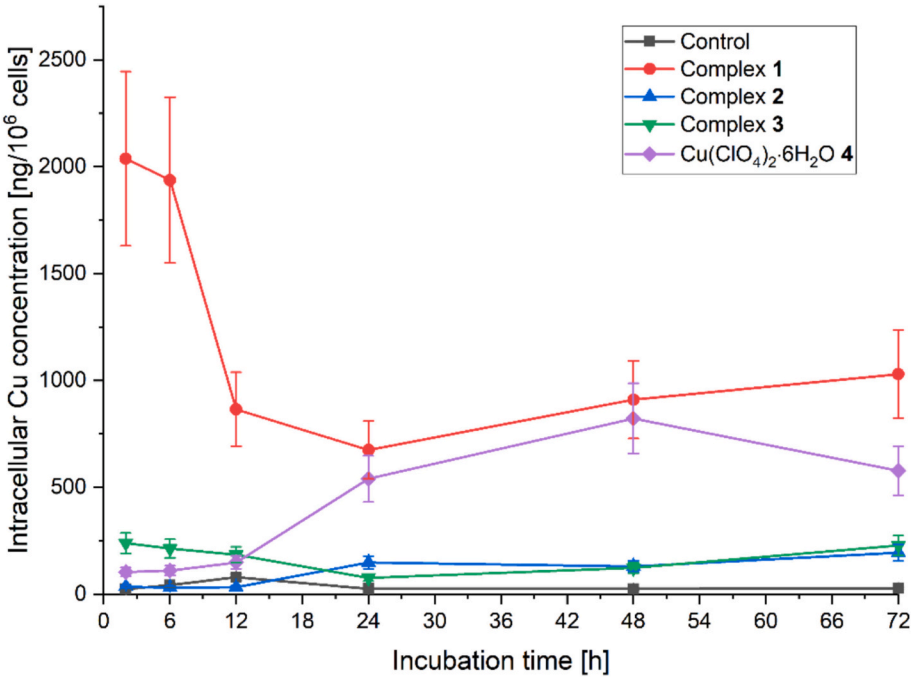

Fig. 2. Intracellular levels of copper in A2780 cells (means ± SD of two independent measurements, μg/10^6 cells), as determined after 2, 6, 12, 24, 48 and 72 h of incubation with complexes **1**–**3** and $Cu(ClO_4)_2{\cdot}6H_2O$ (**4**) using ICP-MS. Vehicle-treated cells were used as control.

atoms are five-coordinated, and one free position can be utilised for DMSO or MeOH molecule bonding. The situation regarding complexes **2** and **3** is different because the maxima observed in the solutions and solid-state spectra are very close, indicating that there proceeds no coordination of the solvent molecule to copper, which also follows from X-ray diffraction results in the case of complex **2**, where only uncoordinated crystal solvent MeOH molecules are present.

2.8. Interaction studies of complexes 1–3 with L-cysteine (Cys) and reduced glutathione (GSH)

To reveal the ability of the complexes **1**–**3** to interact with sulphur-containing biomolecules, the two types of mass spectrometry experiments were performed studying the interactions of 10 μM solutions of complexes **1**–**3** with either 290 μM solution of L-cysteine (Cys), representing the normal serum concentration of this amino acid in the humans, or with 10 mM concentration of GSH (reduced glutathione), representing the maximum known intracellular concentration of reduced glutathione in cells, in MeOH: H_2O (1:1 *v*/v) mixture after 24 h and 72 h of incubation at laboratory temperature. The obtained mass spectra revealed no signals, attributable to interaction products between complexes **1**–**3** and L-cysteine (at ca 30-fold molar excess, see Figs. S23–S28 in Supporting Information) as well as between complexes **1**–**3** and reduced glutathione (at ca. 1000-fold molar excess, see Figs. S29–S34 in Supporting Information) even after 72 h of interaction. Nevertheless, the obtained mass spectra showed that the decompositions of the parent complexes occurred, associated with the liberation of the free ligands and therefore, the corresponding signals of the species $[H_2L + H]^+$ and $[H_2L + Na]^+$, respectively, were identified in the ESI-MS spectra.

Unfortunately, it is not possible to draw clear conclusions regarding the possible mechanism of action of the studied complexes in relation to the obtained biologically-based results. However, in theory, the biological activities of the studied copper(II) complexes **1**–**3** can be related to the inactivation of the enzymatic systems containing these groups (such as peroxidases and peroxiredoxins [39]) or depletion of pools of reducing agents, acting as extracellular and intracellular antioxidants [40], thus causing the metabolic or oxidative stress, which might lead to the activation of some type of the programmed cell death [41].

3. Experimental

The ^{1}H NMR spectra were recorded with 500 MHz Bruker AVANCE-III NMR system. UV/vis–spectra were measured with an Agilent Cary 60 UV/vis spectrophotometer in a 10 mm quartz-glass cuvette. The FTIR spectra were measured with Bruker Optics, Vertex 70 device with a Harrick diamond ATR setup, DTGS detector. 64 scans were performed and all data were recorded in transmittance mode with a resolution of 4 cm^{-1}. In this setup, the sample is pressed against a diamond anvil. The FTIR spectra of ligands **H_2L1**-**H_2L3** and complexes **1**–**3** are shown in Figs. S35-S37 in Supporting Information. The solvents and other chemicals were from commercial suppliers and were used as purchased. All reactions and manipulations were done under an ambient atmosphere. Studies of hydrolysis and interactions with L-cysteine (Cys) and reduced glutathione (GSH) were performed using electrospray ionisation (ESI) mass spectrometry (MS) technique in a positive mode (Bruker amaZon SL, Bruker). The cellular uptake of copper in A2780 cells was determined using the Agilent 7700× inductively coupled plasma mass spectrometer (ICP-MS), using external calibration (Transition metal mix 1 for ICP, Merck). The results were corrected for adsorption effects. UV–Vis spectra of complexes **1**–**3** were measured in DMSO and solutions and in the solid state on a JASCO V-750 UV/VIS spectrometer.

Single crystal X-ray diffraction data of **1** were collected with a Bruker-Nonius Kappa APEX II diffractometer using Mo Kα radiation, while the data of **2** and **3** were collected with a Rigaku diffractometer with a MicroMax-HF source, producing Cu Kα radiation, and a HyPix-6000HE detector. Data collection and reduction of the Rigaku diffractometer were done using the CrysAlis^{Pro} software [42], while COLLECT [43] and HKL Denzo and Scalepack [44] were used for Bruker-Nonius data with the absorption correction applied using SADABS [45]. Crystal structures were solved and refined using SHELXS [46] and SHELXL [47] programs employing the Olex interface [48].

Temperature-dependent (T = 2.5–297 K, B = 0.1 T) magnetic experiments of complexes **1**, **2**, and **3** were performed using a PPMS

Dynacool system (Quantum Design) with a VSM option. The data were corrected for the diamagnetism of the constituents and the sample holder. The magnetic data obtained for the dinuclear complex **1** and trinuclear complex **3** were interpreted using the PHI program package, *ver*. 3.1.6. [32].

The electrochemical experiments were conducted using an Autolab potentiostat. A glassy carbon electrode was used as the working electrode (WE), a platinum coil as the counter electrode (CE), and an Ag/AgCl wire as the reference electrode (REF). Measurements were taken in a special three-neck glass cell. The electrolyte solution (0.1 M) was made using DMSO (99 %) and the electrolyte salt tetrabutylammonium perchlorate (>98 %), as these compounds show good solubility in this solvent system. Dry DMSO and electrolyte salt were used in the experiments, and all solutions were bubbled with N_2 prior to electrochemical measurements. The data is given in Supporting Information, see Figs. S38–40 and Table S3.

The ligand precursors **H_2L1** and **H_2L2** were prepared using the previously published method for synthesising **H_2L3**. [28] 20 mmol of 2,4-disubstituted phenol, 20 mmol (0.60 g) of paraformaldehyde and 10 mmol (1.05 g) of 2-(2-aminoethoxy)ethanol were mixed in the round-bottomed flask, and the reaction mixture was stirred and heated at 125 °C for 4 h. The solid products were crystallised from *n*-hexane-toluene mixture (**H_2L1**) or acetonitrile (**H_2L2**).

H_2L1: Yield: 2.3 g (62 %). ^{1}H NMR ($CDCl_3$): 6.89 (s, 2H, ArH), 6.72 (s, 2H, ArH), 3.86 (t, 2H, J = 3.8 Hz, CH_2OH), 3.70 (s, 2H, $ArCH_2N$), 3.65 (t, 2H, J = 3.8 Hz, CH_2O), 3.61 (t, 2H, J = 6.3 Hz, CH_2O), 2.77 (t, 3H, J = 4.8 Hz, NCH_2), 2.24 (s, 6H, CH_3), 2.23 (s, 6H, CH_3). ^{13}C NMR: 15.88 (p-CH_3), 20.41 (o-CH_3), 51.98 (NCH_2), 56.73 (NCH_2), 61.77 (OCH_2), 68.24 ($HOCH_2$), 73.45 (OCH_2), 121.41 (Ar), 125.09 (Ar), 128.34 (Ar), 129.07 (Ar), 131.25 (Ar), 151.83 (Ar).

H_2L2: Yield: 3.0 g (66 %). ^{1}H NMR ($CDCl_3$): 7.01 (s, 2H, ArH), 6.72 (s, 2H, ArH), 3.85 (t, 2H, J = 4.0 Hz, CH_2OH), 3.74 (s, 2H, $ArCH_2N$), 3.68 (t, 2H, J = 4.8 Hz, CH_2O), 3.66 (t, 2H, J = 4.8 Hz, CH_2O), 2.77 (t, 3H, J = 4.9 Hz, NCH_2), 2.24 (s, 6H, CH_3), 1.38 (s, 18H, $C(CH_3)_3$). ^{13}C NMR: 20.78 (p-CH_3), 29.58 ($C(\underline{C}H_3)_3$), 34.64 ($\underline{C}(CH_3)_3$), 51.95 (NCH2), 57.54 (NCH_2), 61.85 (OCH_2), 68.95 ($HOCH_2$), 73.50 (OCH_2), 122.33 (Ar), 127.42 (Ar), 127.86 (Ar), 128.74 (Ar), 136.87 (Ar), 152.49 (Ar).

General procedure for **1**–**3**. 1.0 mmol (370 mg) of $Cu(ClO_4)_2{\cdot}6H_2O$ was dissolved in 20 ml of MeOH. 1.0 mmol of the ligand precursor (370 (**H_2L1**), 460 (**H_2L2**) or 540 (**H_2L3**) mg) and triethylamine (2.0 mmol, 0.28 ml) were added to obtain a dark, brownish-red solution. The solution was stirred for two hours, filtered, and the volatiles were removed under vacuum to give a dark brown-red solid, which was crystallised from MeOH (**1**, **2**) or *n*-hexane (**3**) and isolated by filtration. The UV–Vis spectra were measured in MeCN, MeOH and a MeOH:H_2O mixture (1:1) on ca. 5×10^{-6} M solutions.

1: Yield: 265 mg (61 %). Calcd. for $C_{44}H_{58}Cu_2N_2O_8$ (M_r = 870.05): C, 60.74; H, 6.72; N, 3.22. Found: C: 60.54; H: 6.81; N: 3.68. IR: 3220 (w, br), 2926 (w), 2862(w), 1602 (w), 1471 (s), 1437 (m), 1377 (w), 1333 (w), 1305 (w), 1245 (s), 1231 (s), 1210 (w), 1166 (w), 1098 (vs), 1065 (vs), 1032 (s), 974 (m), 918 (m), 875 (w), 864 (m), 820 (m), 806 (m), 790 (m), 770 (m), 750 (w), 670 (w), 621 (s), 590 (w), 545 (s), 522 (w), 517 (m), 510 (m), 490 (m), 470 (m). UV–Vis: ε = 1600 cm^{-1} M^{-1} (334 nm), 1400 cm^{-1} M^{-1} (440 nm), 180 cm^{-1} M^{-1}(583 nm). (MeOH): ε = 1350 cm^{-1} M^{-1} (455 nm). (MeOH:H_2O, 1:1): ε = 1170 cm^{-1} M^{-1} (455 nm).

2: Yield: 300 mg (53 %). Calcd. for $C_{32}H_{57}CuNO_8$ (M_r = 647.35): C: 59.37; H: 8.88; N: 2.16. Found: C: 58.92; H: 8.71; N: 2.21. IR: 3585 (w), 2949 (s), 2904 (s), 2862 (s), 1600 (w), 1468 (s), 1437 (vs), 1412 (s), 1385 (w), 1357 (m), 1300 (s), 1278 (s), 1247 (s), 1237 (vs), 1206 (s), 1166 (w), 1151 (m), 1120 (s), 1091 (s), 1069 (s), 1026 (m), 990 (w), 961 (w), 941 (w), 926 (m), 912 (m), 892 (w), 871 (s), 860 (s), 819 (m), 805 (s), 784 (m), 769 (w), 740 (w), 618 (s), 590 (w), 544 (s), 521 (w), 484 (m), 488 (m). UV–Vis: ε = 2300 cm^{-1} M^{-1} (334 nm), 1200 cm^{-1} M^{-1} (513 nm), 400 cm^{-1} M^{-1} (675 nm). (MeOH): ε = 1300 cm^{-1} M^{-1} (488 nm). (MeOH:H_2O, 1:1):): ε = 1160 cm^{-1} M^{-1} (488 nm).

3: Yield: 390 mg (65 %). Calcd. for $C_{108}H_{173}Cu_3N_3O_{12}$ (M_r = 1896.18): C: 68.41; H: 9.20; N: 2.22. Found: C: 68.02; H: 9.14; N: 2.34. IR: 3590 (w), 2948 (s), 2900 (s), 2854(s), 1602 (w), 1470 (s), 1434 (vs), 1415 (s), 1384 (w), 1357 (m), 1298 (s), 1279 (s), 1236 (vs), 1206 (s), 1165 (w), 1150 (w), 1120 (s), 1090 (s), 1068 (s), 1026 (m), 988 (w), 960 (w), 923 (m), 912 (m), 872 (s), 861 (s), 820 (m), 806 (s), 785 (m), 768 (m), 738 (w), 690 (w), 619 (s), 590 (w), 545 (s), 523 (w), 485 (m). UV–Vis: ε = 4400 cm^{-1} M^{-1} (323 nm), 1700 cm^{-1} M^{-1} (518 nm). (MeOH): ε = 980 cm^{-1} M^{-1} (488 nm). (MeOH:H_2O, 1:1):): ε = 1100 cm^{-1} M^{-1} (488 nm).

4. Biological studies

4.1. In vitro cytotoxicity

The cytotoxicity of the complexes **1**–**3** and free ligands (H_2L1−H_2L3) was studied by standard MTT test on a panel of three human cancer cell lines: A2780 (ovarian), A2780R (ovarian, cisplatin-resistant) and MCF7 (breast), together with normal keratinocyte cells (HaCaT). The conventionally used metallotherapeutic drug cisplatin was used as a reference compound. Following the supplier's instructions, the cells were cultivated in 96-well dishes with culture media supplemented with 10 % foetal calf serum. The stock solutions of the tested compounds were prepared immediately before the cell treatment in pure DMF and were further diluted with culture media to achieve final concentrations of 0.1, 1, 10, 25 and 50 μM (containing a maximum of 0.1 % *v*/v DMF) for 24-h treatment. The control cells were treated with vehicle (0.1 % v/v DMF) and the positive control was Triton X-100 (1 %; *v*/v). The standard MTT assay was conducted, and absorbance (A) was measured spectrophotometrically at 570 nm using an Infinite M200 instrument (Schoeller Instruments, Prague, Czech Republic). Data were expressed as the percentage of cell viability, where 100 % and 0 % represent the control cells and positive control, respectively. Half-maximal inhibitory concentrations (IC_{50}) were calculated by fitting dose-response curves using GraphPad Prism 6 software (GraphPad Software, San Diego, USA).

4.2. Copper accumulation in A2780 cells

The half-effective concentrations of complexes **1**–**3**, and $Cu(ClO_4)_2{\cdot}6H_2O$ (**4**) were incubated with A2780 cells at standard growing conditions recommended by the supplier for 2, 6, 12, 24, 48, or 72 h. The control group comprised only the A2780 cells treated by the vehicle (0.1 % v/v DMF-treated cells). After each time period, the cells were detached by trypsinisation, washed twice with PBS (0.1 M, pH 7.4) and isolated by centrifugation. The resulting pellets were digested by 500 μl of concentrated nitric acid for ICP-MS (65 %) and were left to stand at laboratory temperature for 24 h. The volumes of the samples for the ICP-MS analyses were adjusted to 4.5 ml using ultrapure water. The intracellular copper content was determined using the ICP-MS method (ICP-MS spectrometer 7700x, Agilent) and external calibration (Transition metal mix 1 for ICP, Merck). The results were corrected for adsorption effects.

5. Conclusions

The prepared copper(II) complexes (**1**, **2** and **3**) of differently substituted amine-bisphenolates (**H_2L1**, **H_2L2** and **H_2L3**) revealed dinuclear **1**, mononuclear **2** and trinuclear **3** structures. Differences in molecular structures of the complexes also reflect their magnetic features, as complex **1** behaves as a strong antiferromagnet (J = −209 cm^{-1}) and complex **2** behaves as a magnetically diluted paramagnetic compound obeying the Curie-Weiss law. In contrast, complex **3** reveals moderate antiferromagnetic coupling with J_1 = −19.9 (9) cm^{-1}, J_2 = −2.37 (6) cm^{-1}. The compounds showed strong-to-moderate cytotoxicity against human cancer cell lines (ovarian A2780 and A2780R, and breast MCF7). Complexes **2** and **3** are even significantly more effective

against A2780, A2780R and MCF7 cells than the metallodrug cisplatin. Moreover, complexes **1**–**3** also displayed good resistance factors (with RF ≈ 1.1–1.4), while complex **3** demonstrated a good selectivity index (SI) regarding the relationship between cytotoxicity on cancer cells versus normal cells, with SI ≈ 4.8–5.5. The ESI-MS spectra of complexes **1**–**3** in methanol revealed that, under the conditions of electrospray ionisation, complexes dissociate to monomeric species of the general formula $[CuL + H]^+$ or $[CuL + Na]^+$. Complexes **1**–**3** showed no apparent signs of hydrolysis in MeOH/water mixtures after 24 h and 72 h of standing at laboratory temperature. Mass spectrometry-based experiments revealed no formation of the interaction species between **1** and **3** and either L-cysteine (Cys) at *ca* 30-fold molar excess or reduced glutathione (GSH) at *ca* 1000-fold molar excess. However, they revealed a decomposition of the complexes **1**–**3** in these experiments, leading to the liberation of the free ligands and formation of the $[H_2L + H]^+$ and $[H_2L + Na]^+$ species, respectively, as dominant peaks This behaviour may be associated with the resulting cytotoxicity of complexes **1**–**3** against A2780 and A2780R, except for complex **3** on MCF7 cells, where a significant discrepancy between the cytotoxicity of complex **3** and its free **H_2L3** ligands exists.

CRediT authorship contribution statement

Anssi Peuronen: Writing – review & editing, Visualization, Investigation, Formal analysis. **Pia Damlin:** Investigation, Formal analysis. **Ján Vančo:** Writing – review & editing, Writing – original draft, Visualization, Validation, Investigation, Formal analysis, Conceptualization. **Zdeněk Dvořák:** Writing – review & editing, Validation, Methodology, Formal analysis. **Zdeněk Trávníček:** Writing – review & editing, Writing – original draft, Validation, Supervision, Resources, Methodology, Conceptualization, Investigation. **Ari Lehtonen:** Writing – review & editing, Writing – original draft, Validation, Supervision, Resources, Project administration, Conceptualization.

Declaration of competing interest

The authors declare that they have no known competing financial interests or personal relationships that could have appeared to influence the work reported in this paper.

Acknowledgement

The authors would like to thank Ms. Marta Rešová for her help with cytotoxicity testing, Ms. Barbora Komendová for performing UV–Vis experiments, and Mr. Radim Mach for variable-temperature magnetic data acquisition. The authors also thankfully acknowledge the Turku Bioscience Protein Structure and Chemistry Core Facility, a member of Biocenter Finland and FINStruct, for providing access to a single-crystal X-ray diffraction instrument.

Appendix A. Supplementary data

Supplementary data to this article can be found online at https://doi.org/10.1016/j.inoche.2025.115024.

Data availability

Data will be made available on request.

References

[1] T.W. Hambley, Developing new metal-based therapeutics: challenges and opportunities, Dalton Trans. (2007) 4929–4937, https://doi.org/10.1039/B706075K.
[2] K.H. Thompson, C. Orvig, Metal complexes in medicinal chemistry: new vistas and challenges in drug design, Dalton Trans. (2006) 761–764, https://doi.org/10.1039/B513476E.
[3] R. Paprocka, M. Wiese-Szadkowska, S. Janciauskiene, T. Kosmalski, M. Kulik, A. Helmin-Basa, Latest developments in metal complexes as anticancer agents, Coord. Chem. Rev. 452 (2022) 214307, https://doi.org/10.1016/j.ccr.2021.214307.
[4] M. Fanelli, M. Formica, V. Fusi, L. Giorgi, M. Micheloni, P. Paoli, New trends in platinum and palladium complexes as antineoplastic agents, Coord. Chem. Rev. 310 (2016) 41–79, https://doi.org/10.1016/j.ccr.2015.11.004.
[5] A.W.M.A. Schaeffers, M.A. van Beers, L.A. Devriese, F.W.J. Klomp, C.F.M. Westerink - van den Brink, E.J. Smid, R. de Bree, C.M. Speksnijder, How do patients with head and neck cancer and low skeletal muscle mass experience cisplatin-based chemoradiotherapy? A qualitative study, Support Care Cancer 32 (2024) 751, https://doi.org/10.1007/s00520-024-08950-0.
[6] A.L. De Sousa-Coelho, G. Fraqueza, M. Aureliano, Repurposing therapeutic drugs complexed to vanadium in Cancer, Pharmaceuticals 17 (2024) 12, https://doi.org/10.3390/ph17010012.
[7] S. Swaminathan, J. Haribabu, R. Karvembu, From concept to cure: the road ahead for ruthenium-based anticancer drugs, ChemMedChem 19 (2024) e202400435, https://doi.org/10.1002/cmdc.202400435.
[8] M. Hanif, M.V. Babak, C.G. Hartinger, Development of anticancer agents: wizardry with osmium, Drug Discov. Today 19 (2014) 1640–1648, https://doi.org/10.1016/j.drudis.2014.06.016.
[9] J. Shen, T.W. Rees, L. Ji, H. Chao, Recent advances in ruthenium(II) and iridium (III) complexes containing nanosystems for cancer treatment and bioimaging, Coord. Chem. Rev. 443 (2021) 214016, https://doi.org/10.1016/j.ccr.2021.214016.
[10] M.A. Malik, A.A. Hashmi, A.S. Al-Bogami, M.Y. Wani, Harnessing the power of gold: advancements in anticancer gold complexes and their functionalized nanoparticles, J. Mater. Chem. B 12 (2024) 552–576, https://doi.org/10.1039/D3TB01976D.
[11] C. Santini, M. Pellei, V. Gandin, M. Porchia, F. Tisato, C. Marzano, Advances in copper complexes as anticancer agents, Chem. Rev. 114 (2014) 815–862, https://doi.org/10.1021/cr400135x.
[12] R. Tabti, N. Tounsi, C. Gaiddon, E. Bentouhami, L. Désaubry, Progress in copper complexes as anticancer agents, Med. Chem. 7 (2017) 875–879.
[13] D.A. da Silva, A. De Luca, R. Squitti, M. Rongioletti, L. Rossi, C.M.L. Machado, G. Cerchiaro, Copper in tumors and the use of copper-based compounds in cancer treatment, J. Inorg. Biochem. 226 (2022) 111634, https://doi.org/10.1016/j.jinorgbio.2021.111634.
[14] K. Lossow, M. Schwarz, A.P. Kipp, Are trace element concentrations suitable biomarkers for the diagnosis of cancer? Redox Biol. 42 (2021) 101900 https://doi.org/10.1016/j.redox.2021.101900.
[15] A. Gupte, R.J. Mumper, Elevated copper and oxidative stress in cancer cells as a target for cancer treatment, Cancer Treat. Rev. 35 (2009) 32–46, https://doi.org/10.1016/j.ctrv.2008.07.004.
[16] O. Wichmann, R. Sillanpää, A. Lehtonen, Structural properties and applications of multidentate [O,N,O,X'] aminobisphenolate metal complexes, Coord. Chem. Rev. 256 (2012) 371–392, https://doi.org/10.1016/j.ccr.2011.09.007.
[17] O. Wichmann, H. Sopo, E. Colacio, A.J. Mota, R. Sillanpää, A combined experimental and theoretical study on the magnetic properties of a family of Bis (μ-phenoxido)dicopper(II) complexes bearing ω-[Bis(2-hydroxy-3,5-dimethylbenzyl)amino]alkan-1-ol ligands, Eur. J. Inorg. Chem. 2009 (2009) 4877–4886, https://doi.org/10.1002/ejic.200900684.
[18] E. Safaei, T. Weyhermüller, E. Bothe, K. Wieghardt, P. Chaudhuri, A Magnetostructural and electrochemical study of CuII and FeIII complexes containing a Tetradentate Aminebis(phenolate) ligand with a pendent tetrahydrofuran group, Eur. J. Inorg. Chem. 2007 (2007) 2334–2344, https://doi.org/10.1002/ejic.200700095.
[19] Md. Mijanuddin, A.D. Jana, M.G.B. Drew, C.S. Hong, B. Chattopadhyay, M. Mukherjee, M. Nandi, A. Bhaumik, M. Helliwell, G. Mostafa, M. Ali, Concomitant polymorphism of an antiferromagnetically coupled dicopper(II,II) complex with single strand helical assembly: Synthesis, structure, DSC, magnetic and heterogeneous catalytic studies, Polyhedron 28 (2009) 665–672, https://doi.org/10.1016/j.poly.2008.12.047.
[20] A. Rajput, A. Kumar, A. Sengupta, P. Tyagi, H. Arora, Copper (ii) dimers stabilized by bis(phenol) amine ligands: theoretical and experimental insights, New J. Chem. 42 (2018) 12621–12631, https://doi.org/10.1039/C8NJ02591F.
[21] D. Mondal, M.C. Majee, K. Bhattacharya, J. Long, J. Larionova, M.M. Khusniyarov, M. Chaudhury, Crossover from Antiferromagnetic to Ferromagnetic Exchange Coupling in a New Family of Bis-(μ-phenoxido)dicopper(II) Complexes: A Comprehensive Magneto–Structural Correlation by Experimental and Theoretical Study, ACS Omega 4 (2019) 10558–10570, https://doi.org/10.1021/acsomega.8b03656.
[22] E. Safaei, M. Rasouli, T. Weyhermüller, E. Bill, Synthesis and characterization of binuclear [ONXO]-type amine-bis(phenolate) copper(II) complexes, Inorg. Chim. Acta 375 (2011) 158–165, https://doi.org/10.1016/j.ica.2011.04.048.
[23] E. Safaei, A. Wojtczak, E. Bill, H. Hamidi, Synthesis, crystal structure, magnetic and redox properties of Cu(II)–Cu(II) binuclear complexes of bis(phenol) amine ligands, Polyhedron 29 (2010) 2769–2775, https://doi.org/10.1016/j.poly.2010.06.025.
[24] M. Singh, R.J. Butcher, J.P. Jasinski, J.A. Golen, G. Mugesh, Synthesis, characterization and phosphotriesterase mimetic activity of some Zn(II) and cu(II) complexes, J. Chem. Sci. 124 (2012) 1301–1313, https://doi.org/10.1007/s12039-012-0331-4.
[25] Y. Shimazaki, S. Huth, A. Odani, O. Yamauchi, A structural model for the galactose oxidase active site which shows Counteranion-dependent Phenoxyl radical formation by disproportionation, Angew. Chem. Int. Ed. 39 (2000) 1666–1669,

https://doi.org/10.1002/(SICI)1521-3773(20000502)39:9<1666::AID-ANIE1666>3.0.CO;2-O.
[26] Y. Shimazaki, S. Huth, S. Hirota, O. Yamauchi, Studies on galactose oxidase active site model complexes: effects of ring substituents on cu(II)-phenoxyl radical formation, Inorg. Chim. Acta 331 (2002) 168–177, https://doi.org/10.1016/S0020-1693(01)00781-2.
[27] S.S. Massoud, F.R. Louka, N.M.H. Salem, R.C. Fischer, A. Torvisco, F.A. Mautner, J. Vančo, J. Belza, Z. Dvořák, Z. Trávníček, Dinuclear doubly bridged phenoxido copper(II) complexes as efficient anticancer agents, Eur. J. Med. Chem. 246 (2023) 114992, https://doi.org/10.1016/j.ejmech.2022.114992.
[28] M.M. Hänninen, A. Peuronen, P. Damlin, V. Tyystjärvi, H. Kivelä, A. Lehtonen, Vanadium complexes with multidentate amine bisphenols, Dalton Trans. 43 (2014) 14022–14028, https://doi.org/10.1039/C4DT01007H.
[29] A.W. Addison, T.N. Rao, J. Reedijk, J. van Rijn, G.C. Verschoor, Synthesis, structure, and spectroscopic properties of copper(II) compounds containing nitrogen–Sulphur donor ligands; the crystal and molecular structure of aqua[1,7-bis(N-methylbenzimidazol-2′-yl)-2,6-dithiaheptane]copper(II) perchlorate, J. Chem. Soc. Dalton Trans. (1984) 1349–1356, https://doi.org/10.1039/DT9840001349.
[30] M. Llunell, D. Casanova, J. Cirera, P. Alemany, S. Alvarez, SHAPE, version 2.1, Universitat de Barcelona, Barcelona, Spain, 2013.
[31] O. Kahn, Molecular Magnetism, VCH, New York, 1993.
[32] N.F. Chilton, R.P. Anderson, L.D. Turner, A. Soncini, K.S. Murray, PHI: a powerful new program for the analysis of anisotropic monomeric and exchange-coupled polynuclear d- and f-block complexes, J. Comput. Chem. 34 (2013) 1164–1175, https://doi.org/10.1002/jcc.23234.
[33] D. Venegas-Yazigi, D. Aravena, E. Spodine, E. Ruiz, S. Alvarez, Structural and electronic effects on the exchange interactions in dinuclear bis(phenoxo)-bridged copper(II) complexes, Coord. Chem. Rev. 254 (2010) 2086–2095, https://doi.org/10.1016/j.ccr.2010.04.003.
[34] G. Ambrosi, M. Formica, V. Fusi, L. Giorgi, M. Micheloni, Polynuclear metal complexes of ligands containing phenolic units, Coord. Chem. Rev. 252 (2008) 1121–1152, https://doi.org/10.1016/j.ccr.2007.09.027.
[35] S.S. Massoud, F.R. Louka, M.T. Dial, N.N.M.H. Salem, R.C. Fischer, A. Torvisco, F. A. Mautner, K. Nakashima, M. Handa, M. Mikuriya, Magnetostructural properties of some doubly-bridged Phenoxido copper(II) complexes, Molecules 28 (2023) 2648, https://doi.org/10.3390/molecules28062648.
[36] Q. Peña, G. Sciortino, J.-D. Maréchal, S. Bertaina, A.J. Simaan, J. Lorenzo, M. Capdevila, P. Bayón, O. Iranzo, Ò. Palacios, Copper(II) N,N,O-Chelating Complexes as Potential Anticancer Agents, Inorg. Chem. 60 (2021) 2939–2952, https://doi.org/10.1021/acs.inorgchem.0c02932.
[37] D. Trachootham, J. Alexandre, P. Huang, Targeting cancer cells by ROS-mediated mechanisms: a radical therapeutic approach? Nat. Rev. Drug Discov. 8 (2009) 579–591, https://doi.org/10.1038/nrd2803.
[38] M.E. Bravo-Gómez, J.C. García-Ramos, I. Gracia-Mora, L. Ruiz-Azuara, Antiproliferative activity and QSAR study of copper(II) mixed chelate [cu(N–N)(acetylacetonato)]NO3 and [cu(N–N)(glycinato)]NO3 complexes, (Casiopeínas®), J. Inorg. Biochem. 103 (2009) 299–309, https://doi.org/10.1016/j.jinorgbio.2008.10.006.
[39] J. Vašková, L. Kočan, L. Vaško, P. Perjési, Glutathione-related enzymes and proteins: a review, Molecules 28 (3) (2023) 1447, https://doi.org/10.3390/molecules28031447.
[40] L.B. Poole, The basics of thiols and cysteines in redox biology and chemistry, Free Radic. Biol. Med. 80 (2015) 148–157, https:/doi.org/10.1016/j.freeradbiomed.2014.11.013.
[41] K.F. Zahra, R. Lefter, A. Ali, E.C. Abdellah, C. Trus, A. Ciobica, D. Timofte, The involvement of the oxidative stress status in Cancer pathology: a double view on the role of the antioxidants, Oxidative Med. Cell. Longev. (2021) 9965916, https://doi.org/10.1155/2021/9965916.
[42] P.R.O. CrysAlis, Agilent Technologies Ltd, Yarnton, Oxfordshire, England, 2014.
[43] R.W.W. Hooft, COLLECT Nonius BV, Delft, The Netherlands, 1998.
[44] Z. Otwinowski, W. Minor, Processing of X-ray diffraction data collected in oscillation mode, in: C.W. Jr, R.M. Sweet Carter (Eds.), Methods in Enzymology, New York, USA, 1997, pp. 307–326, https://doi.org/10.1016/S0076-6879(97)76066-X.
[45] G.M. Sheldrick, SADABS-2021/1 University of Göttingen, Germany, 1996.
[46] G.M. Sheldrick, A short history of SHELX, Acta Crystallographica Section A Foundations of Crystallography 64 (2008) 112–122, https://doi.org/10.1107/S0108767307043930.
[47] G.M. Sheldrick, Crystal structure refinement with SHELXL, Acta Crystallographica section C, Struct. Chem. 71 (2015) 3–8, https://doi.org/10.1107/S2053229614024218.
[48] O.V. Dolomanov, L.J. Bourhis, R.J. Gildea, J.A.K. Howard, H. Puschmann, OLEX2: a complete structure solution, refinement and analysis program, J. Appl. Crystallogr. 42 (2009) 339–341, https://doi.org/10.1107/S0021889808042726.